OPTIMAL DISCRETIZATION STEPS FOR A CLASS OF SEMI–LAGRANGIAN SCHEMES

Maurizio FALCONE, Roberto FERRETTI and Tiziana MANFRONI

Version: September 30, 1997.

Abstract. We deal with a class of semi–lagrangian high–order approximation schemes for advection equations focusing our attention to the fine tuning of the algorithm. Starting from some a–priori estimates in L^p we analyse how to choose Δt and Δx in order to efficiently obtain accurate results. Interesting features in these schemes are their good accuracy for large time steps and their numerical stability also when the solution is not regular (e.g. discontinuous). We discuss several numerical tests from the point of view of accuracy and efficiency.

Key words. Hyperbolic equations, high–order approximation schemes, semi–langrangian schemes, stability.

AMS(MOS) subject classification. 65M25, 65M15, 65M06.

1. Introduction.

The numerical solution of advection equations is crucial in many applications in computational fluid dynamics where the first order term dominate the diffusion term in a single equation (convection-diffusion problems with low viscosity) and/or as part of a system (Navier-Stokes, Euler). We will then consider the following model problem:

$$\text{(1.1)} \qquad \begin{cases} \dfrac{\partial}{\partial t} v(x,t) = \lambda v(x,t) + f(x) \cdot \nabla v(x,t) + g(x) & \text{in } \Omega \times [0,T] \\ v(x,0) = v_0(x) \end{cases}$$

where Ω is an open subset of $\mathbb{R}^N$, $\lambda \in \mathbb{R}$ and $t \in [0,T]$.

A variety of numerical schemes has been proposed for (1.1). New algoritms have been obtained (see e.g. Douglas and Russell [DR], Hasbani, Livne and Bercovier [HLB], Morton, Priestley and Süli [MPS] and Pironneau [P]) using characteristics, finite elements, finite volumes or a blend of them. The large majority of these methods introduce a viscosity and treat an equation with a "small" second order term. Other schemes, based e.g. on stream–line diffusion, finite differences and semi–lagrangian formulation (see e.g. Johnson–Szepessy [JS], Huges–Mallet [HM], Shu–Osher [SO] and Staniforth-Coté [SC]) do not add diffusion and seem more adequate to solve first order problems. Moreover, these schemes have also been extended to include more general nonlinear problems (although in many cases a precise convergence result is missing).

We will focus our attention on the efficient implementation of a class of semi–lagrangian schemes applied to (1.1). As reported by the literature (see e.g. [SC], [SG], [RW] and references therein), these schemes seem to be expecially appealing for the metereological community which has extensively and successfully used them in massive numerical simulations.

Our idea is that a careful analysis of a model problem can also be useful and valuable when dealing with more complicated issues. Moreover, a precise control of the numerical errors and a correct choice of the discretization steps is crucial to use CPU time at its best. This is crucial in large computations and may greatly increase their feasibility.

We will start our analysis from the theoretical results obtained in [FF1]–[FF2] and, in particular, from a general convergence theorem and a–priori estimates (in $L^\infty(\Omega)$, $L^2(\Omega)$ or pointwise) for the rate of convergence. These estimates depend on the discretization steps in a nontrivial way, so that the result is greatly affected by the relationship between Δt and Δx. The purpose of the present work is precisely to choose this relationship in order to optimize the efficiency of the scheme.

It should be noted that the above analysis remain valid also when the space discretization is made using unstructured grids (which need not to be "adapted" to the vectorfield f) and includes also the effect of the boundary conditions (Dirichlet or periodic).

As numerical experiments show, these schemes usually allow larger time steps than eulerian type schemes. Moreover, they produce good numerical approximations of non smooth solutions also for nonlinear problems (see Section 5).

The outline of the paper is the following. We will review in Section 2 the basic results of the convergence analysis, and show in Section 3 the explicit form (in $\mathbb{R}^1$) of the schemes

used for the numerical tests. In Section 4 we will address the problem of optimizing the performance of the schemes with respect to the convergence rate. The last section contains some numerical test in $\mathbb{R}^1$ and $\mathbb{R}^2$ with a detailed discussion of advantages and disadvantages of different choices of parameters. For a comparison with other algorithms, e.g. on the rotating cone problem, we refer to Tamamidis and Assanis [TA].

2. Construction of the schemes and basic convergence theory.

We will review for reader's convenience the general form of the schemes and some basic results about the order of convergence. We refer to [FF2] for an in–depth theoretical analysis of stability and convergence. On the theoretical side, we just want to point out that the construction of semi–lagrangian schemes is based on the discretization of the representation formula for the solution of (1.1) coupled with some boundary conditions. When we adopt a stationary Dirichlet boundary condition $b(x)$ on $\partial\Omega_{in}$ (the subset fo $\partial\Omega$ where characteristics point inward), the formula is given by

$$v(x,t) = \int_0^{t\wedge\theta(x)} e^{\lambda s} g(y(s))ds + e^{\lambda(t\wedge\theta(x))} v_0(y(t)) \tag{2.1}$$

where $a \wedge b = \min(a,b)$, and

$$\theta(x) := \inf\{t \geq 0 : y(t) \in \mathbb{R}^N \setminus \Omega\}$$

is the so–called "exit time" from Ω for a given point x.

Let φ be a regular function such that Ω is the set of points $\{x : \varphi(x) < 0\}$, $\partial\Omega = \{x : \varphi(x) = 0\}$ and $\varphi(x) > 0$ for $x \notin \overline{\Omega}$. Let us consider the following initial value problem:

$$\begin{pmatrix} \dot{y}(s) \\ \dot{\gamma}(s) \end{pmatrix} = \begin{pmatrix} f(y(s)) \\ e^{\lambda s} g(y(s)) \end{pmatrix} \tag{2.2}$$

with initial conditions $y(0) = x$, $\gamma(0) = 0$. Moreover, consider its one–step discretization:

$$\begin{pmatrix} y_{n+1} \\ \gamma_{n+1} \end{pmatrix} = \begin{pmatrix} y_n \\ \gamma_n \end{pmatrix} + \Delta t \begin{pmatrix} \Phi_f(y_n, \Delta t) \\ \Phi_g(y_n, \Delta t) \end{pmatrix} \tag{2.3}$$

In order to write the Runge–Kutta type scheme (2.3) in a more concise form we define $\Phi(x, \Delta t) = (\Phi_f(x, \Delta t), \Phi_g(x, \Delta t))$.

Let us set a grid with nodes x_j, $j \in Q = \{1, \ldots, q\}$, and let $\{\psi_j(x)\}_{j\in Q}$ be a family of bounded functions such that $\psi_j(x_j) = 1$, $\psi_j(x_m) = 0 \quad (m \neq j)$, $\|\psi_j\|_\infty = 1$. We will use those functions to construct a local (and finite dimensional) representation of our approximate solutions. Several choices are possible, for example finite elements or polynomial bases.

Fix a positive time step Δt, for any grid node we define a "variable time step" η_j as

$$\eta_j := \min\{\{\delta \in \mathbb{R}_+ : \varphi(x_j + \delta\Phi_f(x_j, \delta)) = 0\}, \Delta t\}. \tag{2.4}$$

This practically means that when $x_j + \Delta t\Phi_f(x_j, \Delta t)$ is in Ω, then $\eta_j = \Delta t$. If this is not the case, the time step can be computed looking for the smallest solution of the equation

$$F(\delta) \equiv \varphi(x_j + \delta\Phi_f(x_j, \delta)) = 0 \tag{2.5}$$

that is, the first time–step δ bringing $x_j + \delta\Phi_f(x_j, \delta)$ to the boundary.

We can give now the general form of the schemes,

$$\begin{cases} v_j^n = \Delta t\Phi_g(x_j, \Delta t) + e^{\lambda\Delta t} \sum\limits_{m\in Q} v_m^{n-1}\psi_m(x_j + \Delta t\Phi_f(x_j, \Delta t)) & \text{if } \eta_j = \Delta t \\ v_j^n = \eta_j\Phi_g(x_j, \eta_j) + e^{\lambda\eta_j} b(x_j + \eta_j\Phi_f(x_j, \eta_j)) & \text{if } \eta_j < \Delta t \\ v_j^0 = v_0(x_j) \end{cases} \tag{2.6}$$

which can be rewritten in vector form as

$$V^n = G + \Psi V^{n-1} \tag{2.7}$$

where the definitions for the matrix Ψ and the vector G are obvious by (2.6). Since Ψ is constant, (2.7) gives a very easy and efficient vectorization of the algorithm. Note also that due to (2.4) the second expression in (2.6) can be interpreted as a generalized boundary condition and that there is no need for a structured grid in the first expression.

Remark 2.1: *Computational complexity*
From (2.7) we see that each time step has a complexity of $O(q^2)$, q being the number of nodes. On the other hand, $q = O(1/\Delta x^N)$(N being the dimension of the physical space in (1.1)) when we adopt regular grids (in the sense used in finite element theory). As a consequence the global complexity of the algorithm described by (2.7) is $O(\Delta t^{-1}\Delta x^{-2N})$

Let us quote the main convergence result in [FF2] which will be useful to understand the link between the choice of the discretization steps and the errors. In the statement of the theorem P_k denotes an interpolation operator over the grid and M denotes the symmetric (mass) matrix $M(\psi)$ with entries

$$m_{ij} = \int_\Omega \psi_i(x)\psi_j(x)dx \qquad (i, j = 1, \ldots, q).$$

Theorem 1. *Let the data f, $g \in C^p(\Omega)$ be bounded. Moreover, assume that $v_0 \in W^{1,\infty}(\Omega)$, $\|v(t) - P_k v(t)\|_\infty \le E(k)$ for $t \in [0, \bar{t}]$ () and that the one–step scheme (2.3) is of order p, that is:*

$$|y(\Delta t) - x - \Delta t\Phi_f(x, \Delta t)| \le C\Delta t^{p+1} \tag{2.8}$$

$$\left| \int_0^{\Delta t} e^{\lambda s} g(y(s)) ds - \Delta t \Phi_g(x, \Delta t) \right| \leq C \Delta t^{p+1}. \tag{2.9}$$

Then, the following estimates hold true for some positive constant C:

i) if $\sum_{j \in Q} |\psi_j(x)| \leq 1$, then for any $h < h_0$:

$$\left\| v_h^k(\bar{t}) - v(\bar{t}) \right\|_\infty \leq C \left(h^p + \frac{1}{h} E(k) \right). \tag{2.10}$$

ii) let $|\Psi|_2 \leq 1$ and μ_2 be a positive constant such that $|M(\psi)|_2 \leq \mu_2 k^N$ for any k. Then, for any $h < h_0$,

$$\| v_h^k(\bar{t}) - v(\bar{t}) \|_2 \leq C \left(h^p + \frac{1}{h} E(k) \right). \tag{2.11}$$

■

The second result states that the estimates (2.10), (2.11) hold for a single node x_j with $E(\Delta x)$ denoting the *local* interpolation error in a neighbourhood of x_j, provided the functions ψ_m have support in a ball of radius $O(\Delta x)$ (this is the case for finite elements discretizations) and $\Delta x = o(\Delta t)$. In fact, solutions of (1.1) preserve regularity along characteristics, and as a consequence it turns out that the effect of interpolation errors on singularities is restricted to a radius of $O(\Delta t^p + \Delta x / \Delta t)$ around the singularity. This result allow to improve the estimates (2.10) in the regions of smoothness of the solution (see [FF2] for a more precise statement).

In the following analysis we will always consider the errors in the L^∞ norm since we focus our attention on the pointwise convergence of the algorithm. Clearly, the uniform norm gives also a bound for the L^2 norm.

3. Fully discrete second and third order schemes.

We show in this section an example of construction of schemes based on the coupling between Heun or Runge–Kutta formula and a P_1 or P_2 finite elements base. This choice yields schemes of either second or fourth order with respect to the time step, and of either second or third order with respect to the space step. In order to avoid heavy notations for the base functions, we will restrict to the case of $\Omega = (-1, 1) \subset \mathbb{R}^1$.

Following Heun's formula, we set:

$$\Phi_f(x, \Delta t) = \frac{1}{2} f(x) + \frac{1}{2} f(x + \Delta t f(x)) \tag{3.1a}$$

$$\Phi_g(x, \Delta t) = \frac{1}{2} g(x) + \frac{1}{2} g(x + \Delta t f(x)) e^{\lambda \Delta t}. \tag{3.1b}$$

In the case of the Runge–Kutta scheme we have:

$$K_0 = f(x)$$

$$K_1 = f(x + \Delta t \frac{K_0}{2})$$

$$K_2 = f(x + \Delta t \frac{K_1}{2})$$

$$K_3 = f(x + \Delta t K_2)$$

$$\Phi_f(x, \Delta t) = \frac{1}{6}(K_0 + 2K_1 + 2K_2 + K_3) \tag{3.2a}$$

(3.2b)

$$\Phi_g(x, \Delta t) = \frac{1}{6}(g(x) + 2e^{\lambda \Delta t/2} g(x + \Delta t \frac{K_0}{2}) + 2e^{\lambda \Delta t/2} g(x + \Delta t \frac{K_1}{2}) + e^{\lambda \Delta t} g(x + \Delta t K_2)).$$

The domain Ω may be defined by the inequality $x^2 - 1 < 0$ so that η_j is the minimum between Δt and the smallest positive solution of

$$(x_j + t\Phi_f(x_j, t))^2 - 1 = 0 \tag{3.3}$$

We define

$$z_j := x_j + \eta_j \Phi_f(x_j, \eta_j). \tag{3.4}$$

The simplest choice for the grid is to use equally spaced points, so that the step between the nodes is $\Delta x = 2/(q-1)$ and $x_j = (j-1)\Delta x - 1$. In order to interpolate with P_1 finite elements, the base functions ψ_j should be linear on each subinterval between nodes. It is convenient to define a normalized displacement to obtain always the interpolation from a standard interval (say, $[0, 1)$). To this end, we define

$$k_j := \left[\frac{q-1}{2}(z_j + 1) \right] \tag{3.5}$$

$$\xi_j := \frac{z_j - (k_j \Delta x - 1)}{\Delta x} = \frac{q-1}{2}(z_j + 1) - k_j \tag{3.6}$$

(where $[\cdot]$ denotes the integer part), the point z_j lies in the subinterval $[x_{k_j+1}, x_{k_j+2})$ and $\xi_j \in [0, 1)$ represents the normalized displacement with respect to the point x_{k_j+1}. Then, we have

$$\sum_{m \in Q} v_m^{n-1} \psi_m(x_j + \eta_j \Phi_f(x_j, \eta_j)) = v_{k_j+1}^{n-1}(1 - \xi_j) + v_{k_j+2}^{n-1} \xi_j$$

which gives the discrete approximation:

$$(3.7)\qquad \begin{cases} v_j^n = \Delta t \Phi_g(x_j, \Delta t) + e^{\lambda \Delta t}\left(v_{k_j+1}^{n-1}(1-\xi_j) + v_{k_j+2}^{n-1}\xi_j\right) & \text{if } \eta_j = \Delta t \\ v_j^n = \eta_j \Phi_g(x_j, \eta_j) + e^{\lambda \eta_j} b(z_j) & \text{if } \eta_j < \Delta t \\ v_j^0 = v_0(x_j) \end{cases}$$

with ξ_j, k_j defined by (3.6) and (3.5), z_j by (3.4), η_j by (3.3) and Φ by either (3.1) or (3.2) depending on the time discretization.

To interpolate with P_2 finite elements, q must be an odd number and the functions ψ_j should be quadratic on each subinterval between two subsequent odd nodes. In this case, we define

$$(3.8)\qquad k_j := \left[\frac{q-1}{4}(z_j+1)\right]$$

$$(3.9)\qquad \xi_j := \frac{z_j + 1 - (2k_j+1)\Delta x}{\Delta x} = \frac{q-1}{2}(z_j+1) - 2k_j - 1$$

(here, $z_j \in [x_{2k_j+1}, x_{2k_j+3})$ and $\xi_j \in [-1,1)$). Then, we have

$$\sum_{m\in Q} v_m^{n-1}\psi_m(x_j + \eta_j \Phi_f(x_j,\eta_j)) = v_{2k_j+1}^{n-1}\frac{\xi_j(\xi_j-1)}{2} + v_{2k_j+2}^{n-1}(1-\xi_j^2) + v_{2k_j+3}^{n-1}\frac{\xi_j(\xi_j+1)}{2}$$

which gives the discrete approximation

$$(3.10)\qquad \begin{cases} v_j^n = \Delta t \Phi_g(x_j, \Delta t) + e^{\lambda \Delta t}\left(v_{2k_j+1}^{n-1}\dfrac{\xi_j(\xi_j-1)}{2} + \right. \\ \qquad\qquad \left. + v_{2k_j+2}^{n-1}(1-\xi_j^2) + v_{2k_j+3}^{n-1}\dfrac{\xi_j(\xi_j+1)}{2}\right) & \text{if } \eta_j = \Delta t \\ v_j^n = \eta_j \Phi_g(x_j, \eta_j) + e^{\lambda \eta_j} b(z_j) & \text{if } \eta_j < \Delta t \\ v_j^0 = v_0(x_j) \end{cases}$$

with ξ_j, k_j defined by (3.9) and (3.8), z_j, η_j and Φ as before.

Remark 3.1: *Interpretation as a finite difference scheme*
Even if (3.7), (3.10) are not standard p–points difference schemes, they can still be interpreted as difference schemes, involving for instance (in (3.10)) the points x_j, x_{2k_j+1}, x_{2k_j+2}, x_{2k_j+3}. Looking back at the definition of k_j, it is clear that the stencil of the difference formula enlarges as the time step Δt gets larger. This accounts for the good performances of semi–lagrangian schemes with large time steps, as it has been widely reported by the literature (see e.g. [R], [SP], [SC] and references therein).

4. Relationship between time and space step.

Although the stability of the schemes described in the previous sections is not affected by the magnitude of the time step, a careful choice of Δt is crucial for their performances. In fact, the estimates (2.10), (2.11) show an interplay between Δt and Δx which has to be properly taken into account. We will examine this problem, assuming that the space discretization is piecewise polynomial (of degree r), and that the support of each base function is contained in a ball of radius $O(\Delta x)$. This will allow us to compare the global and the local error. Moreover, we will assume that the solution v has a finite global regularity ($v \in W^{s,\infty}(\Omega)$) but is piecewise C^∞.

First, we can give the following bound for the interpolation error :

$$E(\Delta x) \leq C\Delta x^{\min(s,r+1)} \tag{4.1}$$

Plugging (4.1) respectively into (2.10) (global estimate) and into the corresponding local estimate, if the solution is C^∞ in a small neighbourhood centered at x_j we get,

$$|v_j^n - v(x_j, n\Delta t)| \leq C\left(\Delta t^p + \frac{\Delta x^{\min(s,r+1)}}{\Delta t}\right) \tag{4.2}$$

$$|v_j^n - v(x_j, n\Delta t)| \leq C\left(\Delta t^p + \frac{\Delta x^{r+1}}{\Delta t}\right). \tag{4.3}$$

(we recall that in the latter case, we should assume that $\Delta x = o(\Delta t)$). Our aim is now to express Δt as a function of Δx in the form $\Delta t = \Delta x^\alpha$ and maximize the convergence rate either for (4.2) or for (4.3) with respect to the parameter α.

Minimization of the global error
Using the relationship between the two steps, we obtain

$$|v_j^n - v(x_j, n\Delta t)| \leq C\left(\Delta x^{\alpha p} + \Delta x^{\min(s,r+1)-\alpha}\right) \tag{4.4}$$

so that the convergence rate is $\min(\alpha p, \min(s, r+1) - \alpha)$. Its maximum is attained for

$$\alpha = \frac{\min(s, r+1)}{p+1} \tag{4.5}$$

and it takes the value

$$\alpha p = \frac{p\min(s, r+1)}{p+1}. \tag{4.6}$$

Note that the convergence rate depends crucially on the (global) regularity, and increasing the order of interpolation does not improve the rate (4.6). It should also be noted that the optimal exponent α causes time and space discretizations to affect the error by a similar

order of magnitude. In smooth regions, the convergence rate may not improve since the time discretization error is not related to local regularity.

Minimization of the error in smooth regions
Operating as before, with $s = \infty$, we obtain the optimal exponent

$$\alpha = \frac{r+1}{p+1} \tag{4.7}$$

and accordingly the (local) convergence rate is

$$\alpha p = \frac{p(r+1)}{p+1}. \tag{4.8}$$

However, if $r \geq p$, the condition $\Delta x = o(\Delta t)$ is not satisfied, and therefore the error may not depend only on the local regularity. In conclusion, we have the following cases:

a) for $r < p$, it is possible to apply the local error analysis, obtaining (4.7), (4.8);

b) for $r \geq p$, then two possibilities arise:

b.1) maximize the convergence rate on the basis of the L^∞ estimate;

b.2) set $\alpha = 1 - \varepsilon$ to allow a local improvement of the rate, which will turn out to be $\alpha p = p(1-\varepsilon)$. In fact, when ε decreases, the local convergence rate increases and the region of influence of singularities also becomes larger.

We point out that in the case *b*.1 to have a rate p or higher it is necessary to have a sufficiently regular solution (more precisely, $s > p+1$).

Computational efficiency
It is worth checking that the above choices give the best convergence rate not only with respect to the discretization step, but also with respect to the number of operations (that is, to computing time). Recalling Remark 2.1, and denoting by ν the number of operations, we have

$$\nu = O\left(\Delta t^{-1} \Delta x^{-2N}\right) = O\left(\Delta x^{-(2N+\alpha)}\right).$$

Writing Δx as a function of ν and using it into (4.4), we obtain

$$|v_j^n - v(x_j, n\Delta t)| \leq C\nu^{-\frac{\min(\alpha p, \min(s, r+1)-\alpha)}{2N+\alpha}}. \tag{4.9}$$

An easy computation shows that the absolute value of the exponent in (4.9) is maximized by (4.5) (or (4.7) if $s = \infty$).

5. Numerical tests.

We will compare the theoretical analysis of Section 4 with some numerical results for tests in $\mathbb{R}^1$ and $\mathbb{R}^2$. For each problem, we will consider numerical schemes with a second–order (Heun) or fourth–order (Runge–Kutta) time discretization, coupled with a P_1 or P_2 space discretization, as shown in Section 3. For each scheme, we will consider two relationships between Δx and Δt, which (according to the theoretical analysis) should optimize either the L^∞ or the local error. Moreover, the case $\alpha = 1$ (constant Courant number) will be included in any case for a comparison, since it turns out to be the usual choice in the literature.

Tests 1–6 are related to the following problem:

$$\begin{cases} v_t(x,t) = x v_x(x,t) \\ v(x,0) = v_0(x) = \sin\dfrac{\pi x}{2} \end{cases} \tag{5.1}$$

posed on $[-1,1]$. Its exact solution is

$$v(x,t) = \begin{cases} -1 & \text{if} \quad x < -e^{-t} \\ v_0(e^t x) & \text{if} \quad -e^{-t} < x < e^{-t} \\ +1 & \text{if} \quad x > e^{-t} \end{cases} \tag{5.2}$$

this function is globally $W^{2,\infty}$ but piecewise C^∞.

For each scheme and each relationship $\Delta x/\Delta t$, the errors are computed at $t = 1$ and plotted on a semi–logarithmic scale. In the error table, "local" stands for the error obtained on the interval $[-0.3, 0.3]$ (the solution is C^∞ in this interval), and the order of convergence is computed as

$$\frac{\log(\epsilon_1/\epsilon_2)}{\log(\Delta x_1/\Delta x_2)} \tag{5.3}$$

with Δx_1, Δx_2 chosen as the two extreme steps. The numerical convergence rate is compared with the theoretical rate (in brackets).

For Runge–Kutta/P_1 discretization (Test 1) only the case $\alpha = 2/5$ has been considered, since even with $W^{2,\infty}$ regularity we get the best convergence rate (see (4.1)). The error plot shows that, as expected, the error is not localized; moreover, the convergence rate is very close to the expected value. This also happens for the comparison case $\alpha = 1$ which provides a lower rate.

For Runge–Kutta/P_2 discretization, Test 2 treat respectively the case $\alpha = 2/5$ which is intended to optimize the L^∞ convergence rate, and $\alpha = 3/5$ which should optimize the local convergence rate. The case $\alpha = 1$ is also included for comparison. The rate behaves, at least qualitatively, as expected, but note that the actual convergence rates are always underestimated by the theoretical analysis (see Remark 2.2).

Test 3 is related to Heun/P_2 discretization. For this case, the theoretically optimal relationship is $\alpha = 2/3$ for L^∞ rate and $\alpha = 1$ for local rate. The latter does not ensure

(see section 4) that the assumptions for the local improvement of the convergence rate are fulfilled. However, the radius of the region in which the effect of interpolation errors propagates, is estimated once more by worst–case arguments. In practice, error is distributed in the first case (as expected), and localized in the second case, with rates close to the theoretical ones. Note that, even though the condition $\Delta x = o(\Delta t)$ seems redundant for the local improvement of the convergence rate, still a decrease of the ratio $\Delta x/\Delta t$ causes the error to be more localized (compare the two plots in figure 2). This effect might also be seen in test 2.

Tests 4–6 are related to the so–called 'rotating cone problem', a typical benchmark test in $\mathbb{R}^2$ for the approximation of advection equations (see [SW], [SG], [TA]). The advecting vectorfield is $f(x,y) = (y,-x)$ in $\Omega = (-0.5, 0.5) \times (-0.5, 0.5)$. The initial condition is:

$$v(x,0) = \begin{cases} 1 - \frac{|x-x_0|^2}{r^2} & \text{for } |x - x_0| \le r \\ 0 & \text{elsewhere} \end{cases} \tag{5.4}$$

(with $r = 0.13$) so that the solution is globally Lipschitz continuous and C^∞ outside the curve $|x - x_0| = r$. The errors have been computed at $\bar{t} = 2\pi$, i.e. after one turn around the origin. Moreover, "local" stands here for the error obtained on the ball $|x - x_0| < r/2$ and the convergence rate is again given by (5.3).

In this set of tests we expect that the asymptotic analysis developed in Section 4 applies less precisely, due to the larger discretization steps. In fact, Test 4 seem to give somewhat opposite conclusions: the relationship $\Delta t = \Delta x^{1/5}$, which should optimize the L^∞ error, obtains the best local convergence rate, and vice versa the relationship $\Delta t = \Delta x^{2/5}$ obtains the best L^∞ rate. This does not happen for test 5 and 6 whose behaviour is, at least qualitatively, close to the theoretical forecasts. Note that the local covergence rate in Test 5 is heavily underestimated for $\alpha = 1/5$, but is anyway improved for $\alpha = 3/5$. Note also Test 6 in which the L^∞ error converges despite of the theoretical estimate when $\Delta t = \Delta x$, and the local convergence rate improves the L^∞ rate even if $\Delta t \neq o(\Delta x)$ (see test 3 and again Remark 2.2).

Tests 7–9 are a modification of the rotating cone problem. Here, the initial condition is given again by (5.4), with $x_0 = (-0.2, 0.2)$ and $r = 0.2$, whereas the vectorfield is given by

$$f(x,y) = a(x,y)(y + 0.5, -(x - 0.5))$$

with $a(x,y) = 0.1$ if $(x-0.5)^2+(y+0.5)^2 \le R^2$, $a(x,y) = 0.2$ if $(x-0.5)^2+(y+0.5)^2 > R^2$, R being the distance of x_0 from the point $(0.5, -0.5)$. In practice, the center of the vectorfield is moved to the point $(0.5, -0.5)$, and the vectorfield itself is discontinuous along the circle passing through x_0. The different propagation speeds split the paraboloid into two parts with a discontinuity at the interface. Figure 7 shows the numerical solution of Test 8 at time $t = 4$ and Tables 7–9 contain errors and convergence rates computed again by (5.3) on the extreme steps. The accumulation of interpolation errors is apparent along the discontinuity. However, the local error (computed in the smoothness regions on each side) has a rate of convergence close to those in Tables 4 and 5 (which correspond to a more regular solution). In Test 9 the choice $\alpha = 1$ for the Heun/P_2 scheme gives a lower rate of convergence due to the heavier propagation of interpolation errors for discontinuous solutions.

The last series of tests (10–11) refers to the nonlinear problem (again in $[-1,1]$):

$$\begin{cases} v_t(x,t) + (1-x)v_x(x,t) + 1/2|v_x(x,t)|^2 = 0 \\ v(x,0) = v_0(x) = 1 - x^2. \end{cases} \tag{5.5}$$

The solution of this test problem generates a singularity in the first derivative in a finite time. Moreover, due to the term $(1-x)v_x$, characteristics are curved lines and this makes time discretization important.

A semi–lagrangian technique for the discretization of Hamilton–Jacobi equations like (5.5) is described in [FF1], [FG]. The exact solution of (5.5) can be computed by optimal control arguments and after the onset of a singularity (at $t > \ln\sqrt{2}$) reads

$$v(t,x) \equiv \begin{cases} 0\,, & \text{if } x \le 1 - 2^{-t} \\ (1 - 2\mathrm{e}^{-t} - x)^2 \dfrac{1}{1 - e^{-2t}}\,, & \text{if } 1 - 2\mathrm{e}^{-t} \le x \le 1 - \mathrm{e}^{-t} \\ (1-x)^2 \dfrac{1}{1 - e^{-2t}}\,, & \text{if } 1 - \mathrm{e}^{-t} \le x \le 1 \end{cases}$$

The solution (see Figure 8) shows a discontinuity in the first derivative at $x = 1 - 1/e$ and in the second derivative at $x = 1 - 2/e$. The local error is computed in the interval $[0.4, 0.5]$.

Before examining the results of Tests 10–11, it should be remarked that no "local" version of Theorem 1 is available for this case (and in fact, regularity is not preserved along characteristics in Hamilton–Jacobi equations, as this example shows). Moreover, Theorem 1 itself for the nonlinear scheme is presently proved only for P_0, P_1 space discretizations. In Table 10, L^∞ and local convergence rates are always close one another, local rate being slightly larger. Theoretical forecast is better confirmed by Table 11. Note that the local rate for the case $\Delta t = \Delta x$ is unexpectedly low due to the small error for $\Delta x = 0.04$, but the rate is 1.48 if computed between $\Delta x = 0.02$ and $\Delta x = 0.0025$ and 1.94 between $\Delta x = 0.01$ and $\Delta x = 0.0025$.

Conclusions. We have shown how the theoretical convergence analysis carried out in [FF2] may be applied to optimize the performance of this quite general class of semi–lagrangian schemes. The theoretical results are based on a worst–case analysis and may not always give quantitatively precise results. In particular, the actual convergence rates are usually underestimated by the theoretical ones, and the condition $\Delta t = o(\Delta x)$ for the local improvement of the error seems overly restrictive. However, the following points seem to be confirmed by the numerical experiments:

- optimizing the relationship Δt vs. Δx on the basis of L^∞ error usually gives time and space discretization errors of similar orders of magnitude;
- optimizing the relationship Δt vs. Δx on the basis of local error greatly increases the accuracy in smooth regions;
- the ratio $\Delta x/\Delta t$ is directly related to the radius of the region of reduced accuracy around discontinuities.

Moreover, in the tests presented, the relationship optimizing the local error has usually good performances for L^∞ error as well. In cases where no information about the regularity of solution is available, this is likely to be the best choice for the performance of the scheme. On the other hand, in order to keep the ratio $\Delta x/\Delta t$ low, α should not be too large. This suggests (see (4.7)) that schemes with space discretization of much higher order than time discretization may not be optimal with respect to the local error.

REFERENCES

[DR] J. Douglas Jr. and T. F. Russell, *Numerical methods for convection–dominated diffusion problems based on combining the method of characteristics with finite element or finite difference procedures*, SIAM J. Num. Anal. **19** (1982), 871-885.

[FF1] M. Falcone and R. Ferretti, *Discrete–time high–order schemes for viscosity solutions of Hamilton–Jacobi–Bellman equations*, Num. Math. **67** (1994), 315-344.

[FF2] M. Falcone and R. Ferretti, *Convergence analysis for a class of semi–lagrangian advection schemes*, SIAM J. Num. Anal. **35** (1998), to appear.

[FG] M. Falcone, T. Giorgi, *An approximation scheme for evolutive Hamilton–Jacobi equations*, preprint, 1994.

[HLB] Y. Hasbani, E. Livne and M. Bercovier, *Finite elements and characteristics applied to advection–diffusion equations*, Comput. & Fluids **11** (1983), 71-83.

[HM] T.J. Hughes and M. Mallet, *A new finite element formulation for computational fluid dynamics: IV. A discontinuous–capturing operator for multidimensional advective–diffusive systems*, Comp. Meth. Appl. Mech. **58** (1986), 305-328.

[JS] C. Johnson and A. Szepessy, *On the convergence of a finite element method for a nonlinear hyperbolic conservation law*, Math. Comp. **49** (1987), 427–444.

[Le] R. J. Leveque, *Numerical methods for conservation laws*, Birkhauser, Basel, 1992.

[Li] P. L. Lions, *Generalized solutions of Hamilton–Jacobi equations*, Pitman, London, 1982.

[MPS] K. W. Morton, A. Priestley And E. Süli, *Stability of the Lagrange–Galerkin method with non–exact integration*, RAIRO Model. Math. Anal. Numer. **22** (1988), 625-653.

[P] O. Pironneau, *On the transport–diffusion algorithm and its applications to the Navier–Stokes equations*, Num. Math. **38** (1982), 309-332.

[RM] R. D. Richtmeyer and K. W. Morton, *Difference methods for initial value problems*, Interscience, New York, 1967.

[RW] P.J. Rasch and D.L. Williamson, *On shape–preserving interpolation and semi–Lagrangian transport*, SIAM J. Sci. Stat. Comput. **11** (1990), 656-687.

[R] A. Robert, *A stable numerical integration scheme for the primitive meteorological equations*, Atmos. Ocean. **19** (1981), 35-46.

[SG] P. K. Smolarkiewicz and G.A. Grell, *A class of monotone interpolation schemes*, J. Comput. Phys. **101** (1992), 431-440.

[SP] P. K. Smolarkiewicz and J. A. Pudykiewicz, *A class of semi-Lagrangian approximations for fluids*, J. Atmospheric Sciences **49** (1992), 2082-2096.

[SC] A. Staniforth and J. Coté, *Semi-Lagrangian integration schemes for atmospheric models - a review*, Monthly Weather Review **119** (1991), 2206-2223.

[TA] P. Tamamidis and D. N. Assanis, *Evaluation of various high–order accuracy schemes with and without flux limiters*, Int. J. for Numerical Methods in Fluids **16** (1993), 931-948.

Authors addresses
M. Falcone, Dipartimento di Matematica, Università di Roma "La Sapienza", P.le Aldo Moro, 2, 00185 Roma, Italy, e-mail: falcone @ axcasp.caspur.it
R. Ferretti, Dipartimento di Matematica, Università di Roma "Tor Vergata", v. Fontanile di Carcaricola, 00133 Roma, Italy, e-mail: ferretti @ mat.utovrm.it
T. Manfroni, CASPUR, c/o Università di Roma "La Sapienza", P.le Aldo Moro, 2, 00185 Roma, Italy, e-mail: manfroni @ caspur.it

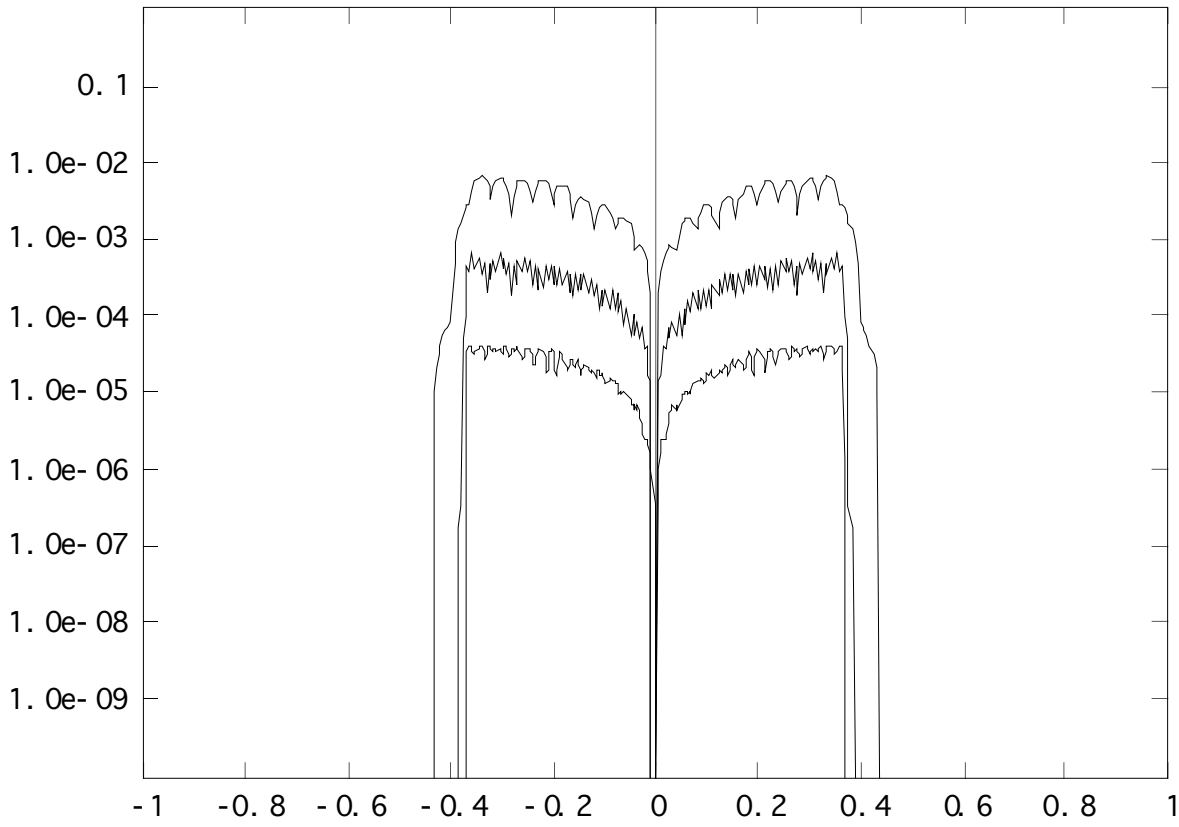

Figure 1: Errors for Test 1, $\Delta x = 0.04, 0.01, 0.0025$, $\Delta t = \Delta x^{2/5}$.

Runge–Kutta/P_1 scheme				
step	$\Delta t = \Delta x^{2/5}$		$\Delta t = \Delta x$	
Δx	L^∞	local	L^∞	local
0.04	$6.58 \cdot 10^{-3}$	$6.18 \cdot 10^{-3}$	$3.33 \cdot 10^{-2}$	$3.33 \cdot 10^{-2}$
0.02	$2.19 \cdot 10^{-3}$	$1.77 \cdot 10^{-3}$	$1.72 \cdot 10^{-2}$	$1.71 \cdot 10^{-2}$
0.01	$6.2 \cdot 10^{-4}$	$5.98 \cdot 10^{-4}$	$8.79 \cdot 10^{-3}$	$8.65 \cdot 10^{-3}$
0.005	$1.36 \cdot 10^{-4}$	$1.33 \cdot 10^{-4}$	$4.45 \cdot 10^{-3}$	$4.34 \cdot 10^{-3}$
0.0025	$4.25 \cdot 10^{-5}$	$4.24 \cdot 10^{-5}$	$2.23 \cdot 10^{-3}$	$2.16 \cdot 10^{-3}$
rate	1.82 (1.6)	1.8 (1.6)	0.98 (1.0)	0.99 (1.0)

Table 1: L^∞ and local errors for Test 1.

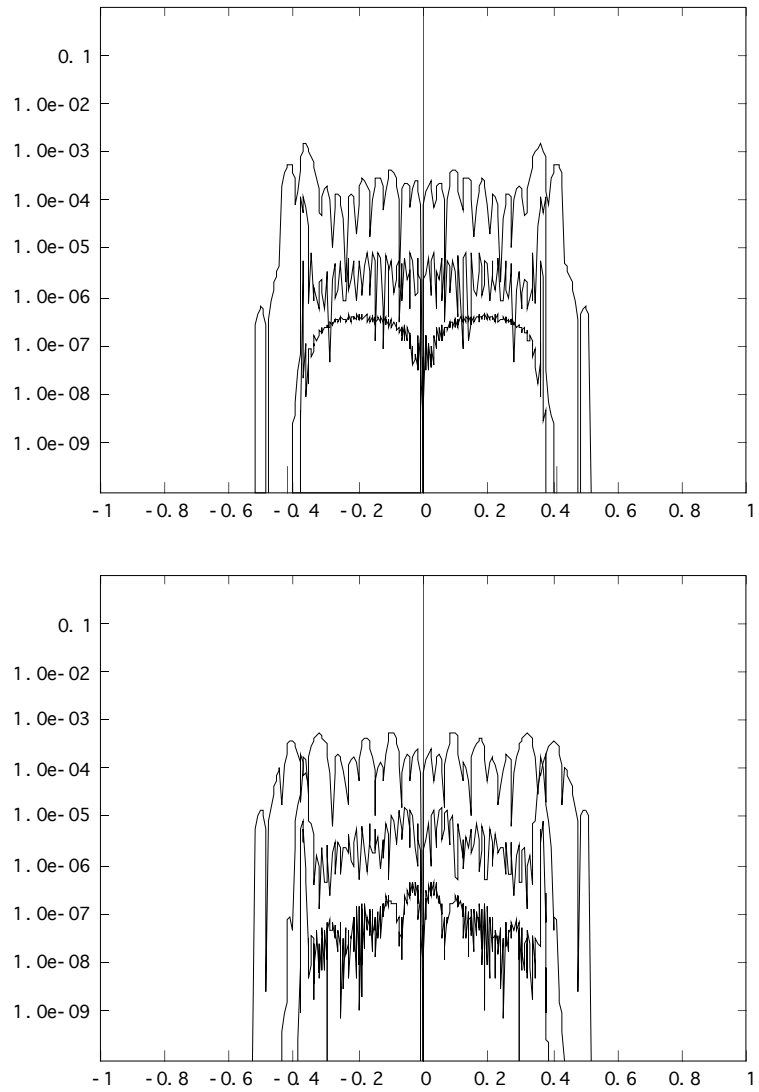

Figure 2: Errors for Test 2, $\Delta x = 0.04, 0.01, 0.0025$, $\Delta t = \Delta x^{2/5}$ and $\Delta t = \Delta x^{3/5}$.

Runge–Kutta/P_2 scheme						
step	$\Delta t = \Delta x^{2/5}$		$\Delta t = \Delta x^{3/5}$		$\Delta t = \Delta x$	
Δx	L^∞	local	L^∞	local	L^∞	local
0.04	$1.47 \cdot 10^{-3}$	$4.36 \cdot 10^{-4}$	$5.88 \cdot 10^{-4}$	$5.48 \cdot 10^{-4}$	$4.47 \cdot 10^{-3}$	$1.01 \cdot 10^{-3}$
0.02	$3.3 \cdot 10^{-4}$	$5.83 \cdot 10^{-5}$	$4.54 \cdot 10^{-4}$	$8.92 \cdot 10^{-5}$	$1.86 \cdot 10^{-3}$	$2.23 \cdot 10^{-4}$
0.01	$1.25 \cdot 10^{-4}$	$8.88 \cdot 10^{-6}$	$1.95 \cdot 10^{-4}$	$1.59 \cdot 10^{-5}$	$7.18 \cdot 10^{-4}$	$5.17 \cdot 10^{-5}$
0.005	$2.8 \cdot 10^{-5}$	$1.44 \cdot 10^{-6}$	$3.12 \cdot 10^{-5}$	$2.45 \cdot 10^{-6}$	$2.78 \cdot 10^{-4}$	$1.23 \cdot 10^{-5}$
0.0025	$6.19 \cdot 10^{-6}$	$4.58 \cdot 10^{-7}$	$7.86 \cdot 10^{-6}$	$4.53 \cdot 10^{-7}$	$1.1 \cdot 10^{-4}$	$2.99 \cdot 10^{-6}$
rate	1.97 (1.6)	2.47 (1.6)	1.53 (1.4)	2.56 (2.4)	1.34 (1.0)	2.1 (2.0)

Table 2: L^∞ and local errors for Test 2.

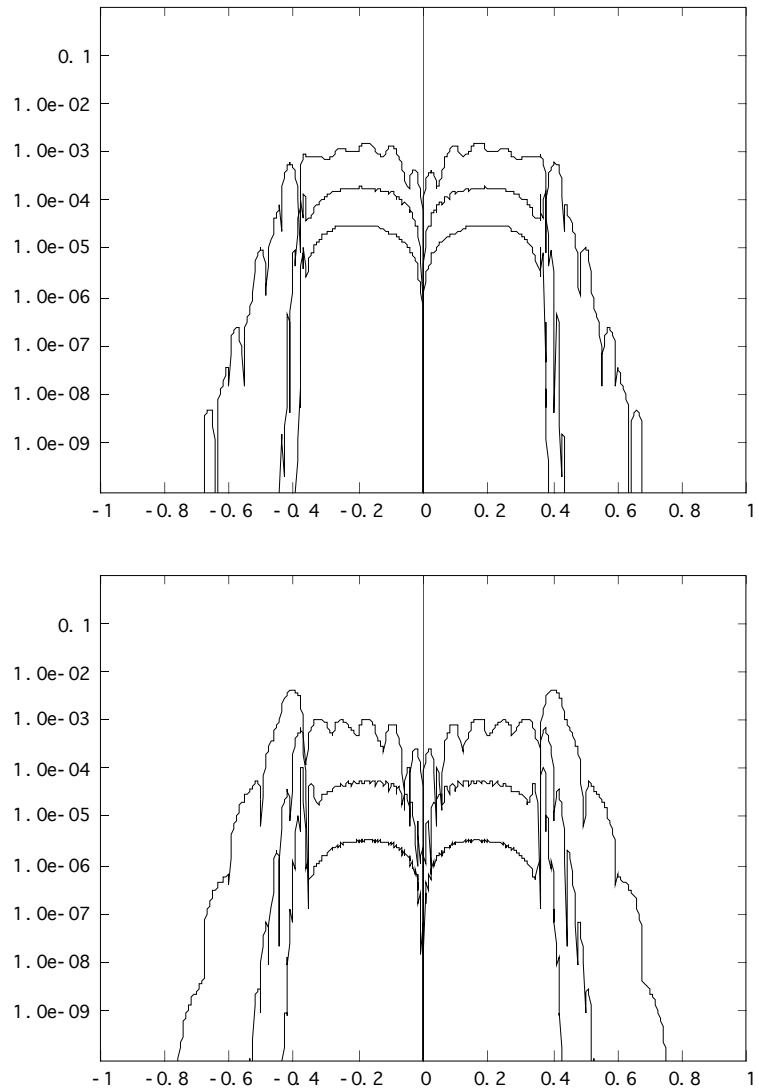

Figure 3: Errors for test 3, $\Delta x = 0.04, 0.01, 0.0025$, $\Delta t = \Delta x^{2/3}$ and $\Delta t = \Delta x$.

Heun/P_2 scheme				
step	$\Delta t = \Delta x^{2/3}$		$\Delta t = \Delta x$	
Δx	L^∞	local	L^∞	local
0.04	$1.6 \cdot 10^{-3}$	$1.6 \cdot 10^{-3}$	$4.48 \cdot 10^{-3}$	$1.15 \cdot 10^{-3}$
0.02	$5.04 \cdot 10^{-4}$	$5.04 \cdot 10^{-4}$	$1.86 \cdot 10^{-3}$	$2.59 \cdot 10^{-4}$
0.01	$1.88 \cdot 10^{-4}$	$1.88 \cdot 10^{-4}$	$7.18 \cdot 10^{-4}$	$6.07 \cdot 10^{-5}$
0.005	$7.85 \cdot 10^{-5}$	$7.85 \cdot 10^{-5}$	$2.78 \cdot 10^{-4}$	$1.45 \cdot 10^{-5}$
0.0025	$3.16 \cdot 10^{-5}$	$3.16 \cdot 10^{-5}$	$1.01 \cdot 10^{-4}$	$3.55 \cdot 10^{-6}$
rate	1.42 (1.33)	1.42 (1.33)	1.36 (1.0)	2.08 (2.0)

Table 3: L^∞ and local errors for Test 3.

Runge–Kutta/P_1 scheme						
step	$\Delta t = \Delta x^{1/5}$		$\Delta t = \Delta x^{2/5}$		$\Delta t = \Delta x$	
Δx	L^∞	local	L^∞	local	L^∞	local
0.04	0.364	0.364	0.519	0.519	0.836	0.836
0.02	0.174	0.129	0.237	0.237	0.781	0.781
0.01	0.0931	0.0359	0.128	0.086	0.630	0.630
rate	0.98 (0.8)	1.66 (0.8)	1.01 (0.6)	1.23 (1.6)	0.2 (0.0)	0.2 (1.0)

Table 4: L^∞ and local errors for Test 4.

Runge–Kutta/P_2 scheme						
step	$\Delta t = \Delta x^{1/5}$		$\Delta t = \Delta x^{3/5}$		$\Delta t = \Delta x$	
Δx	L^∞	local	L^∞	local	L^∞	local
0.04	0.174	0.0685	0.239	0.239	0.546	0.546
0.02	0.132	0.0217	0.176	0.0274	0.338	0.270
0.01	0.0539	0.00413	0.0815	0.00688	0.194	0.0313
rate	0.84 (0.8)	2.03 (0.8)	0.78 (0.4)	2.56 (2.4)	0.75 (0.0)	2.06 (2.0)

Table 5: L^∞ and local errors for Test 5.

Heun/P_2 scheme				
step	$\Delta t = \Delta x^{1/3}$		$\Delta t = \Delta x$	
Δx	L^∞	local	L^∞	local
0.04	0.363	0.281	0.545	0.545
0.02	0.285	0.0974	0.338	0.269
0.01	0.189	0.0543	0.193	0.0312
rate	0.47 (0.66)	1.19 (0.66)	0.75 (0.0)	2.06 (2.0)

Table 6: L^∞ and local errors for Test 6.

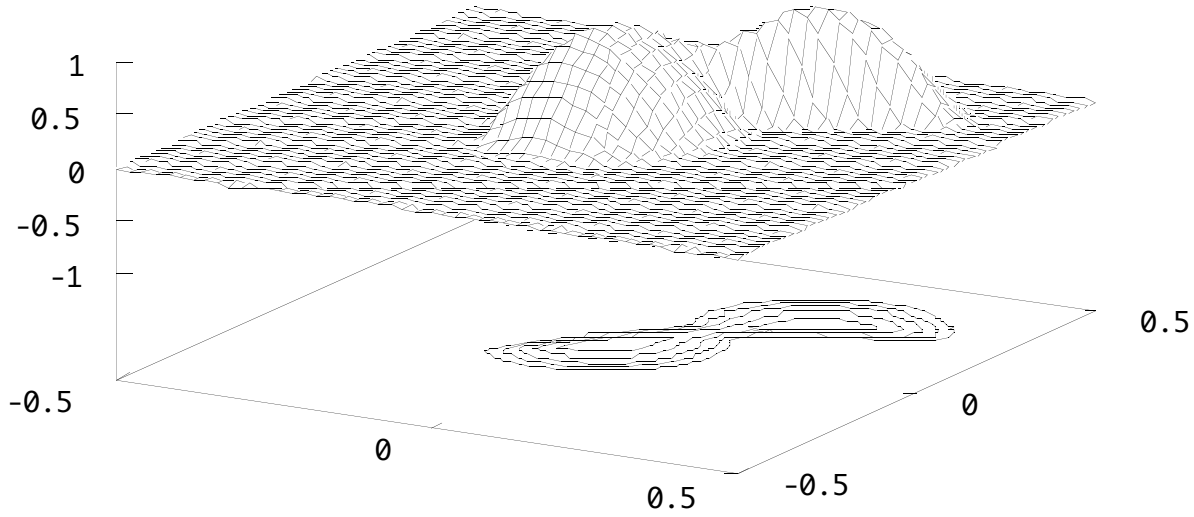

Figure 7: Solution for Test 8 at time $t = 4$, ($\Delta x = 0.01$, $\Delta t = 0.063$).

Runge–Kutta/P_1 scheme				
step	$\Delta t = \Delta x^{2/5}$		$\Delta t = \Delta x$	
Δx	L^∞	local	L^∞	local
0.04	0.508	0.263	0.721	0.498
0.02	0.652	0.127	0.705	0.425
0.01	0.599	0.023	0.698	0.267
rate		1.73 (1.6)		0.45 (1.0)

Table 7: L^∞ and local errors for Test 7.

Runge–Kutta/P_2 scheme				
step	$\Delta t = \Delta x^{3/5}$		$\Delta t = \Delta x$	
Δx	L^∞	local	L^∞	local
0.04	0.606	0.115	0.608	0.166
0.02	0.571	0.036	0.623	0.0314
0.01	0.638	0.0068	0.680	0.045
rate		2.04 (2.4)		0.94 (2.0)

Table 8: L^∞ and local errors for Test 8.

Heun/P_2, $\Delta t = \Delta x$		
Δx	L^∞	local
0.04	0.608	0.165
0.02	0.61	0.031
0.01	0.683	0.045
rate		0.93 (2.0)

Table 9: L^∞ and local errors for Test 9.

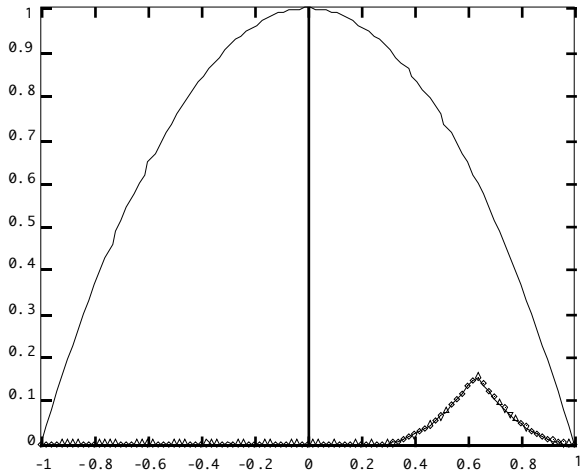

Figure 8: Initial condition, exact and approximate solution ($\Delta x = 0.0833, \Delta t = 0.02$) for Test 11.

Heun/P_1 scheme						
step	$\Delta t = \Delta x^{1/3}$		$\Delta t = \Delta x^{2/3}$		$\Delta t = \Delta x$	
Δx	L^∞	local	L^∞	local	L^∞	local
0.04	$1.9 \cdot 10^{-2}$	$1.25 \cdot 10^{-2}$	$9.08 \cdot 10^{-3}$	$7.59 \cdot 10^{-3}$	$1.55 \cdot 10^{-2}$	$1.16 \cdot 10^{-2}$
0.02	$1.15 \cdot 10^{-2}$	$6.22 \cdot 10^{-3}$	$4.62 \cdot 10^{-3}$	$2.02 \cdot 10^{-3}$	$9.08 \cdot 10^{-3}$	$7.68 \cdot 10^{-3}$
0.01	$8.71 \cdot 10^{-3}$	$4.42 \cdot 10^{-3}$	$1.49 \cdot 10^{-3}$	$1.37 \cdot 10^{-3}$	$5.17 \cdot 10^{-3}$	$4.48 \cdot 10^{-3}$
0.005	$6.35 \cdot 10^{-3}$	$2.9 \cdot 10^{-3}$	$1.39 \cdot 10^{-3}$	$9.07 \cdot 10^{-4}$	$2.93 \cdot 10^{-3}$	$2.29 \cdot 10^{-3}$
0.0025	$3.23 \cdot 10^{-3}$	$1.46 \cdot 10^{-3}$	$5.14 \cdot 10^{-4}$	$3.4 \cdot 10^{-4}$	$1.64 \cdot 10^{-3}$	$1.29 \cdot 10^{-3}$
rate	0.64 (0.66)	0.77 (0.66)	1.04 (0.33)	1.12 (1.33)	0.81 (0.0)	0.79 (1.0)

Table 10: L^∞ and local errors for Test 10.

Heun/P_2 scheme				
step	$\Delta t = \Delta x^{1/3}$		$\Delta t = \Delta x$	
Δx	L^∞	local	L^∞	local
0.04	$1.87 \cdot 10^{-2}$	$1.10 \cdot 10^{-2}$	$3.99 \cdot 10^{-3}$	$1.63 \cdot 10^{-4}$
0.02	$1.15 \cdot 10^{-2}$	$5.93 \cdot 10^{-3}$	$1.3 \cdot 10^{-3}$	$1.01 \cdot 10^{-3}$
0.01	$7.4 \cdot 10^{-3}$	$2.6 \cdot 10^{-3}$	$8.64 \cdot 10^{-4}$	$6.88 \cdot 10^{-4}$
0.005	$5.81 \cdot 10^{-3}$	$2.59 \cdot 10^{-3}$	$1.63 \cdot 10^{-4}$	$8.0 \cdot 10^{-5}$
0.0025	$3.22 \cdot 10^{-3}$	$1.45 \cdot 10^{-3}$	$2.63 \cdot 10^{-4}$	$4.64 \cdot 10^{-5}$
rate	0.63 (0.66)	0.73 (0.66)	0.98 (0.0)	0.45 (2.0)

Table 11: L^∞ and local errors for Test 11.